Development 127, 933-944 (2000)
Printed in Great Britain © The Company of Biologists Limited 2000
DEV2515

Roles of *Hoxa1* and *Hoxa2* in patterning the early hindbrain of the mouse

Jeffery R. Barrow, H. Scott Stadler and Mario R. Capecchi*

Howard Hughes Medical Institute, Department of Human Genetics, University of Utah School of Medicine, Salt Lake City, UT 84112, USA

*Author for correspondence (e-mail: mario.capecchi@genetics.utah.edu)

Accepted 8 December 1999; published on WWW 8 February 2000

SUMMARY

Early in its development, the vertebrate hindbrain is transiently subdivided into a series of compartments called rhombomeres. Genes have been identified whose expression patterns distinguish these cellular compartments. Two of these genes, *Hoxa1* and *Hoxa2*, have been shown to be required for proper patterning of the early mouse hindbrain and the associated neural crest. To determine the extent to which these two genes function together to pattern the hindbrain, we generated mice simultaneously mutant at both loci. The hindbrain patterning defects were analyzed in embryos individually mutant for *Hoxa1* and *Hoxa2* in greater detail and extended to embryos mutant for both genes. From these data a model is proposed to describe how *Hoxa1, Hoxa2, Hoxb1, Krox20* (*Egr2*) *and kreisler* function together to pattern the early mouse hindbrain. Critical to the model is the demonstration that *Hoxa1* activity is required to set the anterior limit of *Hoxb1* expression at the presumptive r3/4 rhombomere boundary. Failure to express *Hoxb1* to this boundary in *Hoxa1* mutant embryos initiates a cascade of gene misexpressions that result in misspecification of the hindbrain compartments from r2 through r5. Subsequent to misspecification of the hindbrain compartments, ectopic induction of apoptosis appears to be used to regulate the aberrant size of the misspecified rhombomeres.

Key words: Hindbrain patterning, *Hoxa1*, *Hoxa2*, *Hoxb1*, *Krox20*, *kreisler*, Mouse, Rhombomere

INTRODUCTION

A recurring theme in embryogenesis is the use of transient compartments to segregate and organize cells en route to the formation of more complex tissues and organs. The embryonic vertebrate hindbrain, for example, is temporarily subdivided into 7 or 8 compartments called rhombomeres which play pivotal roles in the differentiation and segregation of neurons and neural crest along the anteroposterior (AP) axis of the hindbrain (Lumsden and Keynes, 1989). The periodicity of the hindbrain, conferred by segmentation also provides a reference system to coordinate the formation of more peripheral tissues of the head, such as the cranial nerves, craniofacial musculature, and bones. Cells within individual rhombomeres are lineage restricted (i.e., are not free to mix with those of neighboring compartments; Fraser et al., 1990). This segregation provides localized environments for cell-cell interaction and gene activation such that each compartment can then diversify by activation of unique compliment of genes (Hunt et al., 1991a, b).

The fact that the expression patterns of *Hox* genes respect presumptive rhombomere boundaries suggests that, as in *Drosophila*, these genes function to establish the identities of compartments. Indeed, the disruption of *Hoxb1* in the mouse does not cause abnormalities in segmentation of the hindbrain but alters the identity of neurons originating in rhombomere (r) 4 (Goddard et al., 1996; Studer et al., 1996). In addition, *Hoxa2* appears to specify the identity of the mesenchymal neural crest derived from r4. In the absence of *Hoxa2* function, r4-neural crest cells acquire the fate normally associated with neural crest from the anterior segments, r1 and r2 (Gendron-McGuire et al., 1993; Rijli et al., 1993; see also Köntges and Lumsden, 1996). However, unlike the situation in *Drosophila*, *Hox* genes appear to be also involved in the establishment and/or maintenance of segmentation. For example, *Hoxa2* is required to set up the r1/2 boundary as well as to regulate the size of r3 (Gavalas et al., 1997; and herein). *Hoxa1* functions to establish the correct boundaries from r3 through r5 (Lufkin et al., 1991; Chisaka et al., 1992; Carpenter et al., 1993; Mark et al., 1993; Gavalas et al., 1998; and herein). We will argue that the effects of *Hoxa1* mutations on segmentation can be understood in terms of misspecification of rhombomeres.

To further examine the roles of *Hoxa1* and *Hoxa2* during hindbrain segmentation and patterning, we generated mice with a mutant allele that simultaneously disrupts both genes (Barrow and Capecchi, 1999). From an analysis of hindbrains from embryonic day (E) 8.0-E10.5 double mutants, as well as from those individually mutant for *Hoxa1* or *Hoxa2*, a more detailed picture has emerged of how these two genes interact to pattern the rhombencephalon. From these data, a model is developed to explain how *Hoxa1*, *Hoxa2*, *Hoxb1*, *Krox20* and *kreisler* function together to pattern the hindbrain.

MATERIALS AND METHODS

Generation of genotypes

Four different mutant alleles were utilized to generate the mouse embryos described in this study. *Hoxa1*^{neo} (Chisaka et al., 1992) carries an MC1neopA cassette in a *Bgl*II site in the *Hoxa1* homeobox. The *Hoxa1*^{GFP} allele used in this study is described by Godwin et al. (1998). The green fluoresecent protein (GFP) encoding sequences were inserted inframe into the first exon of *Hoxa1*. The *neo* gene, used to select for the ES cell containing the targeted insertion of *GFP*, was subsequently removed from the *Hoxa1* locus by *CRE/loxP* mediated site-specific recombination (Schwenk et al., 1995). The mutant phenotype observed in embryos homozygous for this allele is indistinguishable from those of our *Hoxa1*^{neo} allele (see Chisaka et al., 1992, and Carpenter et al., 1993). The *Hoxa2* mutant allele carries an MC1neopA cassette inserted into the *Hoxa2* homeobox (Barrow and Capecchi, 1999). The fourth allele contains mutations at both the *Hoxa1* and *Hoxa2* loci (*Hoxa1*^{cla}*Hoxa2*^{neo}). This allele is identical to *Hoxa2*^{neo}, with the addition of a *Cla*I linker, frameshift mutation in the *Hoxa1* homeobox at the *Bgl*II site. The PCR conditions and primer used for genotyping are described by Barrow and Capecchi (1999).

RNA in situ hybridization

RNA in situ hybridization was performed as described previously (Manley et al., 1995). Probes were as follows: *Hoxb2*, a 900 bp fragment that extends from a site 130 bp upstream of the stop codon into the 3′UTR; *EphA4*, a 1.2 kb cDNA clone (Gilardi-Hebenstreit, 1992); *neuregulin*, a 2.2 kb cDNA clone (Meyer et al., 1997); *follistatin*, a 300 bp *Bam*HI/*Hin*cII fragment (Albano et al., 1994).

Immunohistochemistry

Krox20 and Hoxb1 double labeling was performed with Hoxb1 and Krox20 antibodies described previously (Manley and Capecchi, 1995 and Goddard et al., 1996). Embryos were preblocked in PBSTM (2% powdered milk, 0.5% Triton X-100 in PBS) at room temperature for 2× 1 hour. The embryos were incubated with a 1:150 dilution of rabbit anti-Hoxb1 antibody in PBSTM at 4°C overnight followed by washes as described above. The embryos were then simultaneously incubated overnight but with a Texas Red-conjugated donkey anti-rabbit secondary antibody (Molecular Probes, Eugene Oregon). The embryos were washed and again incubated O/N with a 1:200 dilution of horseradish peroxidase-conjugated donkey anti-rabbit secondary antibody. This incubation was performed in order to saturate the Hoxb1 antibodies with anti-rabbit antibodies. The embryos were washed and incubated overnight with a 1:100 dilution of rabbit Krox20 antibody, washed, and incubated overnight with a 1:200 dilution of FITC-conjugated, donkey anti-rabbit secondary antibody (Jackson Immunolabs). Finally, the embryos were washed, rinsed, and stored in PBS. The Texas Red- and FITC-conjugated antibodies were visualized through rhodamine and fluorescein filter sets, respectively, with a laser scanning BioRad MRC1240 confocal microscope. The Hoxa1gfp/Hoxb1 immunohistochemistry experiments were visualized in precisely the same manner.

The positions of rhombomere boundaries in Fig. 3 were defined by the following means: 3 control embryos that had been doubly stained for Krox20 and Hoxb1 were imaged as described above; the rhombomere boundaries, as defined by these two markers, were drawn on the images (in Photoshop™) as well as the anterior boundary of the first somite for each of the embryos. Using the somite boundary as a reference point, these measurements were superimposed and then averaged. Similar measurements were taken except using the flexure in the mesencephalon as an external reference point. Both of the averaged measurements were superimposed on the mutant embryos shown in Fig. 3.

TUNEL analysis

Embryos were fixed in 4% paraformaldehyde PBS for 2 hours at room temperature and washed 3× 30 minutes in PBS containing 1% Triton X-100 (PBST). The embryos were preincubated for 30 minutes at 37°C in 1× terminal transferase buffer (Boehringer Mannheim). The buffer was removed and replaced with 1× terminal transferase buffer, 0.5 units terminal transferase/μl, and 10 μM dUTP (2:1 ratio of dUTP:dUTP-biotin). The reaction in this mixture was allowed to proceed for 3 hours at 37°C. The terminal transferase product was quantified by reaction with Texas Red-conjugated streptavidin and viewed by confocal microscopy. Following the TUNEL procedure, some of the embryos were embedded in paraffin and sectioned at 7 μm. The sections were mounted on Superfrost + (Fisher) slides and cleared in 10% glycerol/PBS.

RESULTS

Both the *Hoxa1* and *Hoxa2* single mutants exhibit defects in the organization of rhombomeres in the developing hindbrain (Carpenter et al., 1993; Mark et al., 1993; Gavalas et al., 1997, 1998; Studer et al., 1998). We examined the organization of rhombomeres in each of the single mutants in greater detail to allow comparison with the *Hoxa1/Hoxa2* double mutants. By crossing mice carrying the *Hoxa1* or *Hoxa2* mutations to those harboring the double mutant allele, we generated mice with intermediate genotypes (*Hoxa1*$^{-/-}$*/Hoxa2*$^{+/-}$ and *Hoxa1*$^{+/-}$*/Hoxa2*$^{-/-}$). The hindbrain patterning defects of mutants

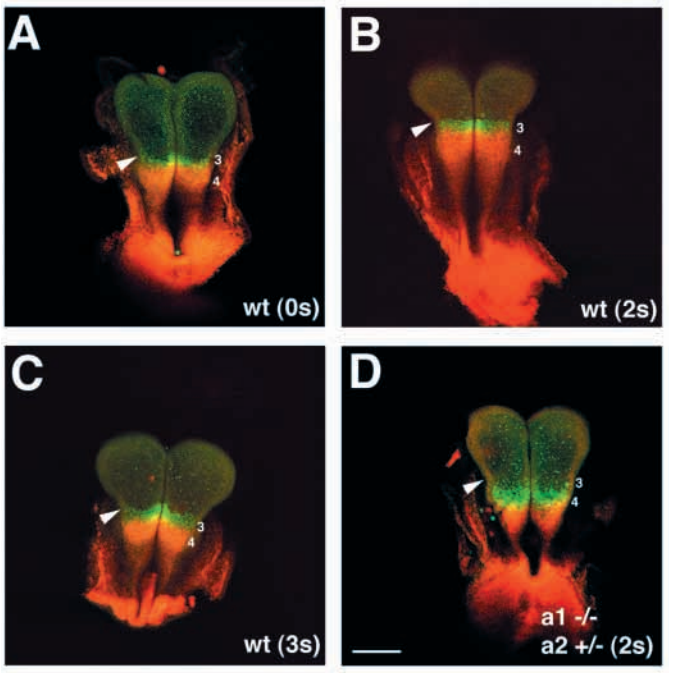

Fig. 1. Labeling of Krox20 and Hoxb1 in E8.0 (0-3 somites) embryos. Krox20 is detected with an FITC-conjugated antibody (green) while Hoxb1 is detected with a Texas Red-conjugated antibody (red). The white numbers indicate the rhombomere number; arrowheads delineate the preotic sulcus (r2/r3 boundary). (A-C) Wild-type control embryos at the 0, 2 and 3 somite (s) stages, respectively. Note the expansion of the *Krox20* in r3 and the intensification of Hoxb1 in r4 as the embryo ages. (D) A *Hoxa1*$^{-/-}$*/Hoxa2*$^{+/-}$ embryo at the 2 somite (2s) stage. The Krox20 domain of expression is mainly at the level of r4. There are very few Krox20-expressing cells just posterior to the preotic sulcus at the level of r3. Dorsal views; scale bar 200 μm.

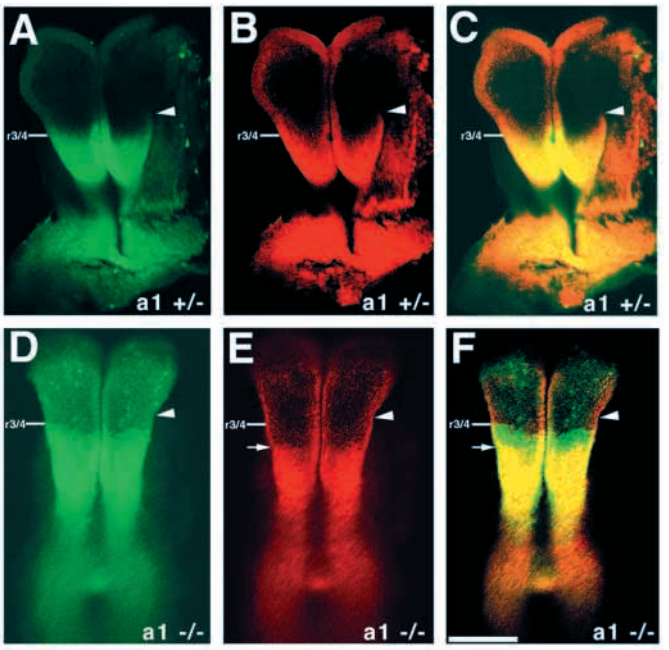

Fig. 2. Hoxb1 expression is shifted caudally relative to *Hoxa1* expression in *Hoxa1* mutants. (A-C) *Hoxa1gfp*$^{+/-}$ embryo at the 2-3 somite stage. (A) Visualization of Hoxa1gfp. The anterior limit of expression defines the r3/4 boundary which is approx. 1 rhombomere length below the preotic sulcus (arrowhead). (B) Hoxb1 immunostaining of the same embryo. (C) Visualization of both Hoxa1gfp and Hoxb1 expression; note that the anterior limits of expression exactly coincide. (D-F) *Hoxa1gfp*$^{-/-}$ embryo at the 3 somite stage. (D) Visualization of Hoxa1gfp; note that the anterior limit of expression of *Hoxa1* (r3/4) is approximately the same distance from the preotic sulcus (arrowhead) as in controls. (E) Hoxb1 immunostaining of the same embryo. The anterior limit of Hoxb1 expression (arrow) is not well defined and is well below the preotic sulcus as well as the anterior limit of Hoxa1gfp expression. (F) Visualization of Hoxa1gfp and Hoxb1 immunostaining; note the significant distance between the anterior limit Hoxa1gfp expression (green; r3/4) and that of Hoxb1 (yellow; arrow). Scale bar, 200 μm.

possessing these intermediate genotypes were not distinguishable from those of mice carrying only the respective single mutations (i.e., *Hoxa1*$^{-/-}$ mice were indistinguishable from *Hoxa1*$^{-/-}$/*Hoxa2*$^{+/-}$ mice; *Hoxa2*$^{-/-}$ mice were similar to *Hoxa1*$^{+/-}$/ *Hoxa2*$^{-/-}$ mice).

Hoxa1 is required to establish the anterior limit of *Hoxb1* expression

We first examined expression of Hoxb1 and Krox20 in E8.0 control and *Hoxa1* mutant embryos. As expected, in control embryos at the 0 somite stage Hoxb1 is expressed in the posterior neural tube to a precise anterior limit at the presumptive r3/4 boundary (Fig. 1A; Frohman et al., 1990; Murphy and Hill, 1991). In addition, Krox20 expression is seen in a narrow band, 3-4 cell diameters in width, in presumptive r3 (Fig. 1A; see also Schneider-Maunoury et al., 1993). At the

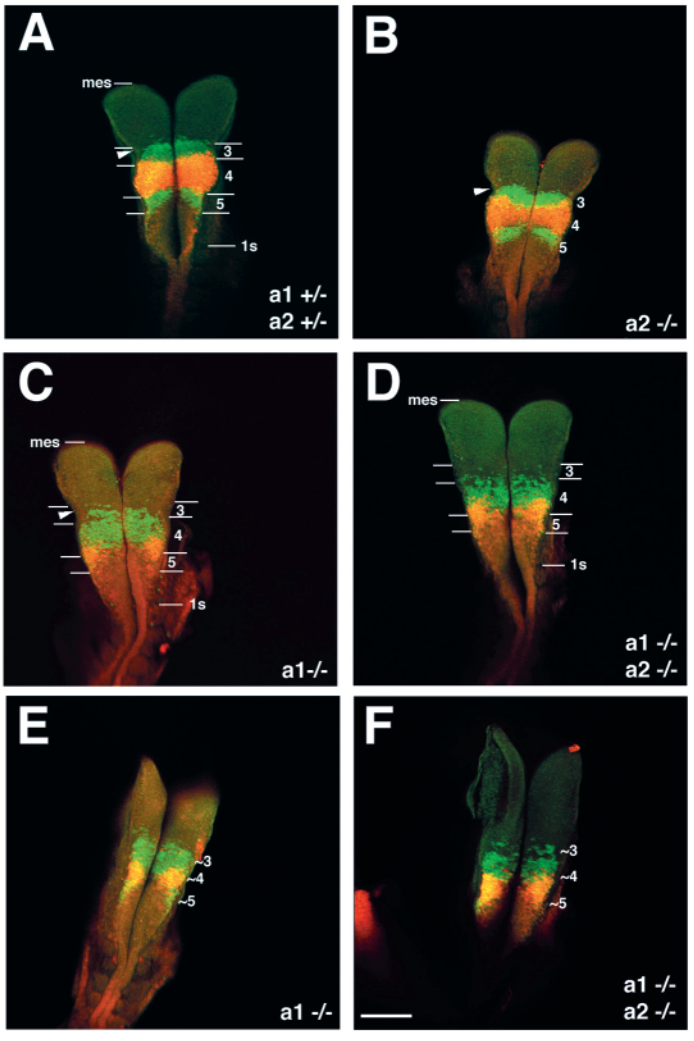

Fig. 3. Labeling of Krox20 and Hoxb1 in E8.5 embryos (4.5-7 somites). The numbers indicate the rhombomere; arrowheads indicate the preotic sulcus. Krox20 expression is visualized using FITC (green) and Hoxb1 using Texas-Red (red). For A, C and D, distances from the flexure in the mesencephalon (mes) or the first somite (1s) to each of the rhombomere boundaries were measured and averaged in 3 age-matched control embryos, and superimposed on each of the embryos shown (Materials and Methods). The embryo in B was not age-matched. (A) Control embryo (*Hoxa1*$^{+/-}$/*Hoxa2*$^{+/-}$) at the 5 somite stage; note the strong expression of Krox20 in r3 and r5 and of Hoxb1 in r4. The dorsal cells (perhaps premigratory neural crest) posterior to r5 are just beginning to express Krox20. (B) *Hoxa2* mutant at the 4-5 somite stage; note the Hoxb1-expressing cells in the lateral-most portions of r3. (C) *Hoxa1* mutant at the 5 somite stage; Krox20 expression is patchy in r3. This expression extends into the r4 region. Only scattered cells at the level of r5 express Krox20. Hoxb1 expression is found in caudal r4 and into r5 (D) *Hoxa1/Hoxa2* double mutant at the 5 somite stage; very similar to age matched *Hoxa1* mutants except that there are very few Krox20-expressing cells at the level of r3. (E) *Hoxa1* mutant at 6-7 somites; Krox20 expression has expanded more fully and is less patchy than at earlier stages. (F) *Hoxa1* and *Hoxa2* double mutant at the 6-7 somite stage. The Krox20 expression has expanded, although somewhat weakly, into the r3 domain (relative to double mutants at earlier stages). Scale bar, 200 μm.

2-3 somite stage, the Hoxb1 expression level increases in the presumptive r4 region, and the Krox20 expression domain extends anteriorly (Fig. 1B,C). The anterior limit of Krox20 expression corresponds to the position of the preotic sulcus (Fig. 1, arrowhead), an indentation in the hindbrain that delineates the r2/3 boundary (Trainor and Tam, 1995). Hoxb1 expression in r4 coincides with a bulge in the hindbrain (Figs 1A-C, 3A,B). Using the positions of the preotic sulcus and the 'r4 bulge' as points of reference in *Hoxa1* mutants, however, the anterior limit of Hoxb1 expression is shifted caudally, to the posterior end of this bulge (Fig. 1D). Krox20 expression was also shifted caudally such that it was found at the level of r4, and only a few cells expressing Krox20 were observed in the region just posterior to the preotic sulcus, which in wild-type embryos would correspond to r3. Thus, in the absence of *Hoxa1*, it appears that the anterior limit of Hoxb1 is established at a more posterior level. Perhaps as a consequence of this posterior shift in Hoxb1 expression, Krox20 expression is also found at a more caudal level.

To directly confirm the posterior shift of Hoxb1 expression in *Hoxa1* mutants, we took advantage of a second allele of *Hoxa1* that has a GFP cassette inserted in frame into the *Hoxa1* encoding unit. In this allele, GFP-fluorescence recapitulates, with high fidelity, *Hoxa1* expression in embryos either heterozygous or homozygous for the *Hoxa1* mutation (Godwin et al., 1998). In heterozygous control, E8.25 embryos, the anterior limits of *Hoxa1* (GFP-green fluorescence) and Hoxb1 (immunohistochemistry-red fluorescence) expression coincide at the r3/r4 presumptive boundary (Fig. 2A-C). However, in *Hoxa1* mutant homozygotes, Hoxb1 expression does not reach the same anterior limit of expression as *Hoxa1*, and is instead observed to be expressed almost one rhombomere caudal to this boundary (Fig. 2D-F). Thus, *Hoxa1* gene activity is required to establish the normal anterior limit of expression of Hoxb1 at the r3/r4 presumptive boundary. Note that in *Hoxa1* mutants, within the region that no longer expresses Hoxb1, neither paralogous gene is functional, placing this region in double jeopardy.

Hoxb1 and Krox20 expression was then examined at E8.5. In control embryos at E8.5 (4-7 somites), Krox20 expression was observed, as expected, in rhombomeres 3 and 5 and Hoxb1 was found in r4 (Fig. 3A; Wilkinson et al., 1989; Murphy and Hill, 1991). Again, the anterior limit of Krox20 expression in r3 aligns with the preotic sulcus and Hoxb1 expression is restricted to the r4 bulge. The Krox20 expression domain in r5 is at the level of the otic sulcus, a second indentation in the hindbrain that delineates the r5 region (Murphy and Hill, 1991). Thus, as is the case at E8.0, the Hoxb1 and Krox20 expression boundaries correspond to morphological landmarks within the hindbrain. The expression of these genes was not significantly altered in *Hoxa2* single mutants (Fig. 3B). In *Hoxa1* mutants, however, the expression patterns are again very different relative to control embryos (Fig. 3C). In spite of these differences in Hoxb1 and Krox20 expression, the *Hoxa1* mutant hindbrains did not differ in length from the hindbrains of age-matched controls and they possessed similar morphological structures such as the preotic sulcus and the r4 bulge. In order to allow the superimposition of the rhombomere boundaries normally associated with wild-type embryos onto *Hoxa1* and *Hoxa1/Hoxa2* mutant embryos, we measured the distances from the preotic sulcus, the mesencephalic flexure and the first somite to the Hoxb1 and Krox20 expression boundaries in three age-matched (5 somite) wild-type embryos (Fig. 2A and data not shown). These distances were averaged and then superimposed onto age-matched *Hoxa1* and *Hoxa1/Hoxa2* mutant embryos (Fig. 3C and D and data not shown) using the morphological markers as the points of reference (Materials and Methods).

As in *Hoxa1* mutants at E8.0, those at E8.5 expressed Krox20 in the region of the hindbrain that would have given rise to r4 in control embryos. In contrast to the earlier mutants, however, the Krox20 domain had expanded more significantly into the region immediately caudal to the preotic sulcus or 'r3' (Fig. 3C). By E8.75, the Krox20 expression rather than being patchy in the preotic region was more confluent in appearance (Fig. 3E). Thus, the expansion of the Krox20 expression at the level of r3 is reminiscent of that observed in control embryos 12 hours earlier (see Fig. 1A-C). We also observed that the Hoxb1 expression domain was very reduced relative to controls, that its anterior limit was at the level of posterior r4, but that it extended abnormally into r5 and beyond. By E8.75, we observed Krox20 expression in the dorsal neuroepithelium at the level of caudal r5 and r6 (Fig. 3E). In control embryos, we observed similar expression in the dorsal portion of r6 at E8.75 (data not shown; to a lesser extent at E8.5-Fig. 3A). It is therefore possible that these cells in the mutant represent the dorsal r6 expression seen in normal embryos, but may also be a remnant of the r5 Krox20-expressing domain.

At E8.5, *Hoxa1/Hoxa2* double mutant embryos had a Krox20 staining pattern that is similar to that of *Hoxa1* single mutants, except that it is restricted to the region in the hindbrain that would typically give rise to r4 (Fig. 3D) and very few expressing cells at the level of r3. At E8.75, double mutants had some small patches of expressing cells in the 'r3' region (Fig. 3F) demonstrating that the expansion of Krox20 expression into r3 is further delayed relative to *Hoxa1* single mutants. Although the preotic sulcus and r4 bulge are difficult to appreciate in the specimen exhibited in Fig. 3D, it should be noted that other double mutants did possess these morphological landmarks and the expression patterns of Krox20 and Hoxb1 were consistent with those shown here. The specimens shown here were chosen because they were precisely age-matched (5 somites) to the controls used in this study. The Hoxb1 expression domain in double mutants corresponds to the posterior r4/anterior r5 region of age-matched control embryos, similar to the finding in *Hoxa1* single mutants. Interestingly, a similar caudal extension of *Hoxb1* expression has been reported for *kriesler* mutants (McKay et al., 1994). It is therefore possible that *kreisler* may be misregulated in mutants that lack *Hoxa1* (see below).

To further explore the perturbations in the organization of rhombomeres in the early hindbrain of *Hoxa1*, *Hoxa2* and *Hoxa1/Hoxa2* mutant embryos the expression patterns of additional molecular markers of the hindbrain were examined.

neuregulin and *follistatin* expression

In E9.0 control embryos, *neuregulin* is expressed strongly in rhombomeres 2 and 4 (Meyer et al., 1997) and at lower levels in r1 (Fig. 4A). *Hoxa2* mutants show a relatively indistinguishable pattern of *neuregulin* expression from controls. In both controls and *Hoxa2* mutants the r4 expression stripe was in perfect alignment with the second branchial arch

(Fig. 4A,B) whereas the otic placode was found immediately posterior to this domain at the level of r5. In *Hoxa1*$^{-/-}$ mutants, the nonexpressing region caudal to r2 was much larger than in control embryos, which corresponds to the large *Krox20*-expressing region observed in embryos at slightly earlier stages of embryogenesis (Fig. 4C). In addition, a thin stripe of *neuregulin* expression is observed that was posterior to the second branchial arch and adjacent to the otic placode. By these morphologic criteria the second *neuregulin* stripe corresponds to the region that would normally give rise to r5 in wild-type embryos. *Hoxa1/Hoxa2* double mutants exhibit a *neuregulin* expression pattern reminiscent of *Hoxa1* mutants. Again the second *neuregulin* stripe is posterior to the second branchial arch and at the level of the otic placode. Thus, as appeared to be the case at earlier stages of embryogenesis, the misspecification of r4 identity at the level of r5 is confirmed at E9.0 in mutants lacking *Hoxa1*. There were two major differences in the double mutants relative to *Hoxa1* single mutants. First, the nonexpressing region between the *neuregulin*-expressing stripes was much smaller in the double mutants. Second, the anterior boundary of this nonexpressing region was patchy. We suggest that the basis for this difference in expression is most likely due to the severe delay in the expression of *Krox20* in r3 of the double mutants (see Fig. 3D,F). Hence in the absence of *Krox20* expression at the level of r3, these cells take on an r2 identity. Indeed, it has been reported by Helmbacher et al. (1998), that in *Hoxa1*$^{-/-}$/*Krox20*$^{+/-}$ mutant embryos which have patchy *Krox20* expression in r3, those cells that do not express *Krox20* take on an r2 identity.

A more direct molecular mechanism is revealed by examining *follistatin* expression in the mutant embryos. At E8.0, *follistatin* is expressed to an anterior limit at the presumptive r1/r2 boundary down through rhombomere 4 as well as in the paraxial mesoderm (Albano et al., 1994). This large expression domain is broken up by a thin stripe of nonexpression in presumptive r3 which by E8.5 has expanded more completely. Thus, there are two bands of expression in r2 and r4 separated by a nonexpressing region in r3 (see Fig. 4E and Albano et al., 1994). In *Krox20* mutants, *follistatin* is expressed from rhombomeres 2-4, demonstrating that *Krox20* directly or indirectly represses the expression of *follistatin* (Seitanidou et al., 1997). Based on this data, it is not surprising that we find a large region of the hindbrain that does not express *follistatin*, which corresponds to the large *Krox20*-expressing domain in *Hoxa1* mutant embryos (Fig. 4G). In *Hoxa1/Hoxa2* double mutants, there is also a relatively large nonexpressing region, the anterior most portion of which, is intermixed with expressing cells (Fig. 4H). Given that *Krox20* represses *follistatin*, we suggest that this patchy *follistatin* expression in r3 of double mutants would be secondary to the severely affected *Krox20* expression at this level of the hindbrain. In mutants lacking *Hoxa1*, we also remarked that the second *follistatin* band was very thin (Fig. 4G,H; sometimes difficult to appreciate due to the underlying expression in the paraxial mesoderm). An interpretation for this very thin 'r4' band is that *follistatin* is typically expressed in rhombomeres 2-4 excepting in r3 where *Krox20* represses its expression. In mutants lacking *Hoxa1*, however, we have provided evidence that the *Krox20* expression domain extends ectopically into the anterior portion of r4 (Figs 1D, 3D-F). Thus, *follistatin* will be repressed in the anterior-most portion of the rhombomere, leaving only a narrow stripe of expression in posterior r4.

Hoxb2 and *EphA4* expression

To further examine the consequences of the misexpression of *Hoxb1* and *Krox20* on later hindbrain development, the expression of *Hoxb2* and *EphA4*, which serve as markers of rhombomeres 3-6 at E9.5, were determined. At this stage *Hoxb2* is expressed strongly in r3-5, to a lesser extent in r6, and at lower levels in the remaining neural tube (Fig. 5A; Sham et al., 1993; Barrow and Capecchi, 1996). In addition, neural crest cells emanating from r4 and r6 express this gene. In *Hoxa2* mutants, *Hoxb2* expression is identical to that of control littermates except that the dorsal-most aspect of r3 is more restricted (Fig. 5B and data not shown). In *Hoxa1*$^{-/-}$ embryos, r3, or the region defined by the anterior limit of *Hoxb2* expression, and the ensuing rhombomere sulcus (designated by the arrowhead in Fig. 5C) appeared only slightly larger than in controls. This observation is in contrast to younger embryos in which an unusually large region of the hindbrain expresses r3 markers. The next segment, which we termed the r4/r6 region, appeared to be one large segment expressing *Hoxb2* at high levels (r5 is assumed not to be present due to the fact that at earlier stages in development a region of the hindbrain that expresses r5 markers is not observed in these mutant embryos; see also Carpenter et al., 1993). Neural crest cells expressing *Hoxb2* were not detected emanating from this large segment.

Hoxa1/Hoxa2 double mutants showed several significant changes relative to the other mutant classes. First, we observed an ill-defined anterior limit of *Hoxb2* expression (Fig. 5D). Interestingly, this limit extended to the bulge in the hindbrain that typically corresponds to the midpoint of r2 in control embryos. In addition, the region of the hindbrain expressing high levels of *Hoxb2* anterior to the otic vesicle (presumably r3) were greatly reduced relative to controls and to the other mutant classes. Expression in the r4/r6 region was strong, as in *Hoxa1* mutants; however, there was no well-defined posterior limit of expression. Instead, the expression faded in gradient fashion.

In control embryos at E9.5, *EphA4* is expressed strongly in r3 and r5 and at lower levels in r2, 4, and 6 (Gilardi-Hebenstreit et al., 1992; Fig. 5E). In *Hoxa2*$^{-/-}$ mutants, the *EphA4* expression pattern is similar to that of controls except that the A-P extent of r3 has been reduced and its anterior limit of expression (r2/3) is ill-defined (Fig. 5F). In *Hoxa1* mutants, a single band of expression was seen anterior to the otic vesicle that represents the r3 region (Fig. 5G). As was demonstrated in *Hoxa1* mutants in the previous experiment, this 'r3' domain is not significantly larger than the r3 band of controls. In addition, the r5 band is not present, presumably due to the fact that r5 markers were never expressed. As was the case in *Hoxa1* homozygotes there is a single band of expression anterior to the otocyst in the *Hoxa1/Hoxa2* double mutants (Fig. 5H). In the double mutants, however, the *EphA4* expression is much more patchy and is restricted to the dorsolateral ridge plate and was found to extend to the mid-point of r2, similar to the *Hoxb2* expression pattern (Fig. 5H; arrow). Thus, it is clear from *Hoxb2* and *EphA4* expression in the double mutants that by E9.5 there is a clear reduction in the size of the r2-r5 region of the hindbrain.

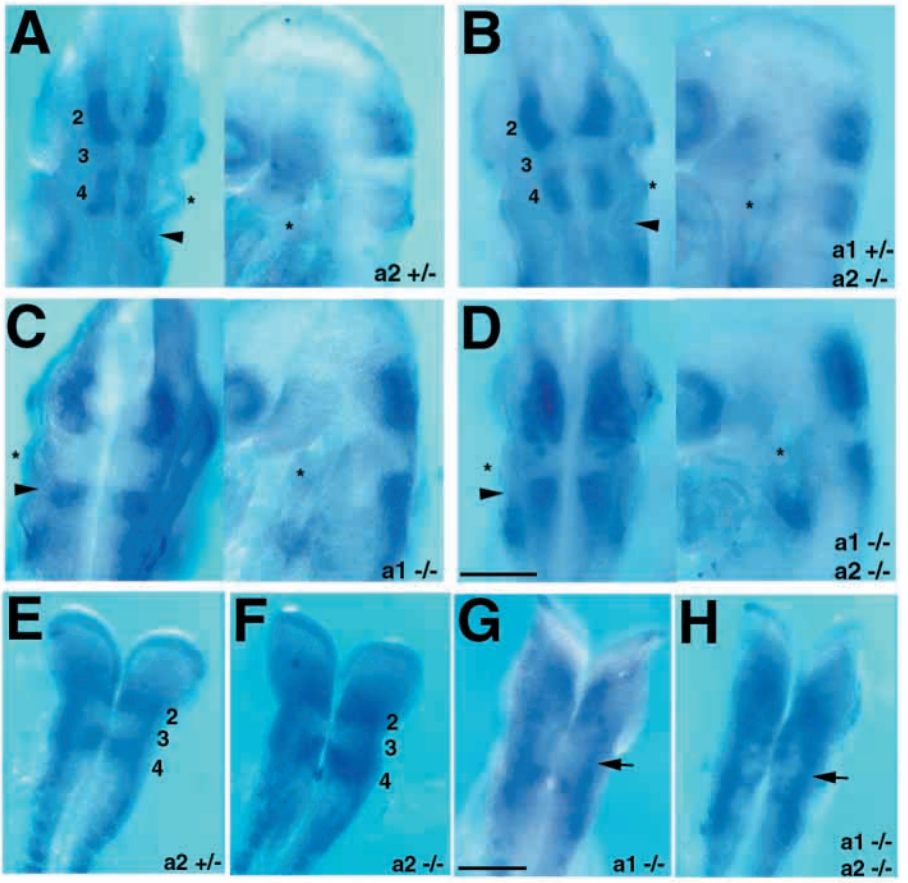

Fig. 4. *Neuregulin* and *follistatin* expression in the hindbrains of mutant embryos. (A-D) *Neuregulin* expression in E9.0-9.25 embryos, shown in both dorsal and lateral views. (A) Control embryo at E9.25; strong expression is seen in r2 and 4, with light expression in r1, 3 and 5. The r4 stripe is directly dorsal to the second branchial arch (*) and immediately anterior to the otic placode (arrowhead). (B) *Hoxa1*$^{+/-}$/*Hoxa2*$^{-/-}$ embryo; appears essentially identical to wild type; not the position of the r4 stripe relative to the decond branchial arch (*) and otic placode (arrowhead) is not altered in this mutant background. (C) *Hoxa1* mutant; the non-expressing region posterior to r2 is much larger and continues into r4 as evidenced by the fat that it is directly above the second branchial arch (*). The Hsecond neuregulin stripe is posterior to the second branchial arch and is adjacent to the otic placode, consistent with it being at the the level of r5. (D) *Hoxa1/Hoxa2* double mutant; the r3 region is composed of both expressing and non-expressing cells. As was the case with *Hoxa1* single mutants, the r4 stripe is posterior to the second branchial arch (*) and adjacent to the otic placode (arrowhead). (E-H) *follistatin* expression in E8.5-8.75. (E) Control embryo (*Hoxa2*$^{+/-}$); *follistatin* is expressed strongly in r2 and 4 and in the cranial and somitic paraxial mesoderm. (F) *Hoxa2* mutant; essentially identical to the control embryo. (G) *Hoxa1* mutant; expression is still seen in two bands in r2 and r4; however, they are separated by an abnormally large nonexpressing domain which appears to extend through much of r4 (arrow). As a consequence, the second *follistatin* stripe is very thin. (H) *Hoxa1/Hoxa2*$^{-/-}$; the nonexpressing region (arrow) is not as confluent and is smaller than the corresponding region in *Hoxa1* single mutants corresponding to the smaller, patchy *Krox20* expression observed in contemporary embryos (see Fig. 3F). This region like that of the single mutants does appear, however, to extend into r4 as demonstrated by the thin 'r4' stripe. Scale bars are 200 μm.

Enlarged rhombomeres in *Hoxa1* mutants are regulated by apoptosis

At E8.5, *Hoxa1* mutant embryos possess an abnormally large segment of the rhombencephalon that expresses r3 molecular markers, which by E9.5 is reduced to almost normal proportions. Extensive TUNEL assays were performed on *Hoxa1* mutants and controls from E8.5 to E10.5 to determine whether apoptosis is used to regulate this abnormally large segment. At E8.5, there were increased, ectopic levels of apoptosis in the anterior hindbrain of *Hoxa1* mutants relative to age matched control embryos (data not shown; see also Rossel and Capecchi, 1999). By E9.0-9.5 (20-22 somites), we observed a peak in the level of apoptosis in the hindbrain from approximately r3 and further anterior (Fig. 6B,D). Although more concentrated at the dorsal aspect of the neural epithelium, apoptotic cells were found along the entire dorsoventral axis of the neural tube (Fig. 6D, inset). Following E9.5, the ectopic apoptosis in the anterior hindbrain decreased such that by E10-10.5 the levels were similar to those of wild-type embryos (data not shown). Like *Hoxa1* single mutants, we found that *Hoxa1/Hoxa2* double mutants also exhibited elevated levels of apoptosis in the hindbrain in early embryogenesis (data not shown).

Hoxa1 and *Hoxa2* have overlapping functions in the formation of rhombomere boundaries

The rhombomeric boundaries in the hindbrain can be visualized with Nomarski optics (Gavalas et al., 1997). In E10.0-10.5 control embryos, the boundaries separating r1-r6, as well as the otocysts adjacent to the r5/6 region are readily observed (Fig. 7A). *Hoxa2* mutants lack two rhombomere boundaries: r1/r2 and r2/r3 (Fig. 7B). This finding is similar yet more severe than data reported by Gavalas et al. (1997) who observed the absence of the r1/r2 and occasionally the r3/4 boundaries with their *Hoxa2* allele. It has been previously shown that our *Hoxa1* mutants lack r5 (Carpenter et al., 1993). Supporting these data, *Hoxa1* mutants were found to have one less rhombomere than control littermates (see Fig. 7C). We also found that the otocyst is positioned at the level of r4 (Fig. 7C; Carpenter et al., 1993; Mark et al., 1993). We suggest that this is likely due to the fact that r4 is specified adjacent to the otocysts (Fig. 4C), rather than to the otocysts being shifted anteriorly to r4. *Hoxa1/Hoxa2* double mutants were found to have completely smooth hindbrains devoid of any boundaries at all stages examined (Fig. 7D). Thus, *Hoxa1* and *Hoxa2* appear to have synergistic roles in the specification of both the anterior and posterior rhombomere boundaries.

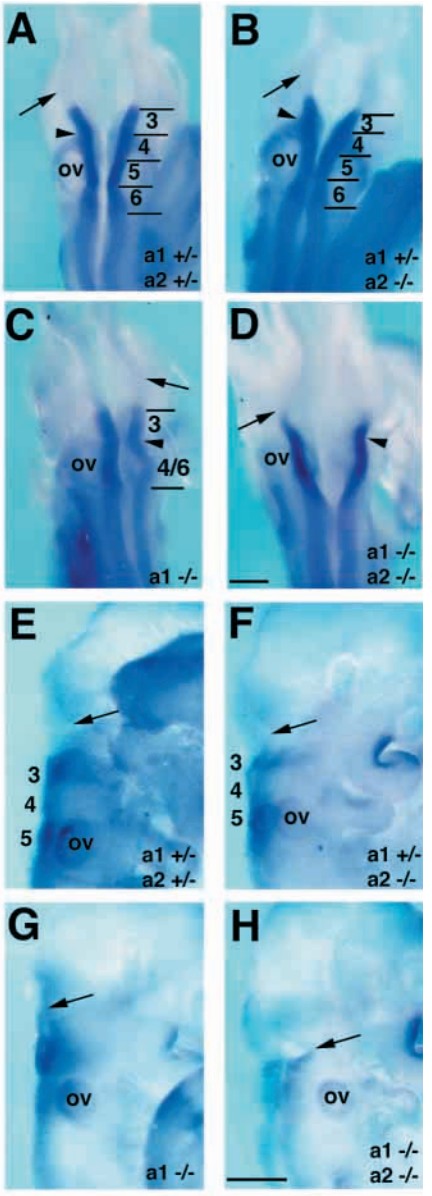

Fig. 5. *Hoxb2* and *EphA4* expression in mutant embryos at E9.5. (A-D) *Hoxb2* RNA expression in E9.5 embryos (dorsal views). The arrows point to the flexure marking the midpoint of r2 whereas the arrowheads indicate the sulcus separating r3 and r4. (A) Control embryo (*Hoxa1*$^{+/-}$/*Hoxa2*$^{+/-}$); strong expression is seen in r3-5 and slightly lower levels in r6. It is also seen in the neural crest emanating from r4 and r6. Note the distance between the midpoint in r2 (arrow) and the r2/3 boundary. (B) *Hoxa1*$^{+/-}$*Hoxa2*$^{-/-}$ mutant; expression pattern is indistinguishable from control embryos except that the r2/3 boundary is ill defined and r3 appears reduced in size. (C) *Hoxa1*$^{-/-}$ embryo; there are two segments of *Hoxb2* expression: one in r3 which is slightly larger than controls and in the r4/6 region. No neural crest is observed from the r4/6 segment. (D) *Hoxa1*$^{-/-}$/*Hoxa2*$^{-/-}$ double mutant embryo. The 'r3' expression domain (i.e., anterior to the r3/4 sulcus; arrowhead) is much smaller than controls and appears to extend into r2 (arrow). The distance between r2 and the otic vesicle is markedly reduced relative to the other mutant classes and controls. Posterior to the r3/4 sulcus, the expression pattern is similar to *Hoxa1* mutants except that there is no sharp posterior border of expression. (E-F) *EphA4* RNA expression in E9.5 embryos (lateral views). (E) Control embryo (*Hoxa1*$^{+/-}$/*Hoxa2*$^{+/-}$) exhibits strong expression in r3 and r5; the anterior limit of expression at the r2/3 boundary is well separated from the midpoint in r2 (arrow). (F) *Hoxa*$^{+/-}$/*Hoxa2*$^{-/-}$ embryo possesses a reduced r3 expression domain. (G) *Hoxa1* mutant with a slightly larger r3 expression domain but lacking the r5 expression stripe. The otic vesicle is adjacent to r4 (or *EphA4* non-expressing cells). (H) *Hoxa1/Hoxa2* double mutant; the anterior limit of expression extends to the midpoint in r2 (arrow). The region between the midpoint of r2 and the otic vesicle has been drastically reduced relative to controls and other mutant classes but does continue to express *EphA4*, albeit weakly. There is no r5-expressing domain. ov, otic vesicle. Scale bars are 200 μm.

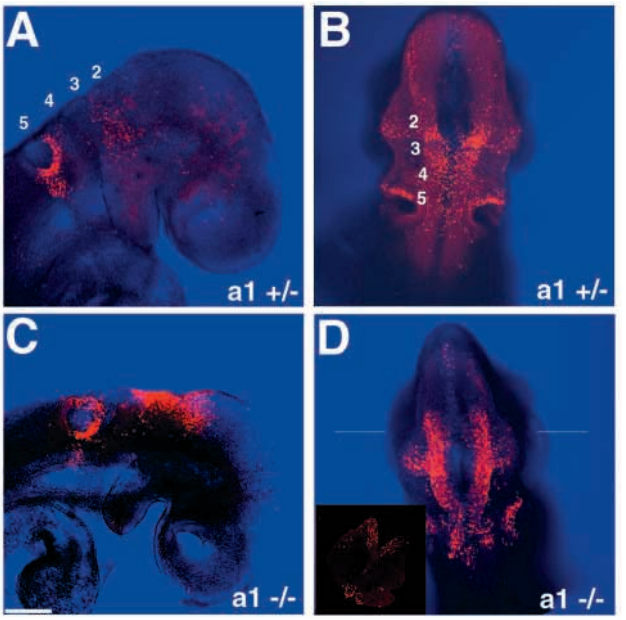

Fig. 6. Apoptosis in the anterior hindbrain of E9.0 embryos. Lateral (A) and dorsal (B) views of a control embryo (+/-); observe the low levels of apoptosis in the anterior hindbrain and moderate levels in r5 and the otocyst. Lateral (C) and dorsal (D) views of a *Hoxa1*$^{-/-}$ embryo; note the extensive apoptosis in the anterior hindbrain. The inset is a transverse section of the embryo in D. The line shows the axial level of the section. Note that the apoptotic cells are found throughout the dorsoventral extent of the neural tube. Scale bar is 200 μm.

DISCUSSION

We have shown that in *Hoxa1* mutants the anterior boundary of *Hoxb1* expression does not reach the presumptive r3/r4 boundary. We suggest that as a consequence of the loss of *Hoxa1* and *Hoxb1* activity at the level of r4, a cascade of gene misexpression ensues that results in misspecification of the hindbrain compartments encompassing r2 through r5. We now review data from previous work, relate it to the results of the present study and propose a model describing how *Hoxa1*, *Hoxb1*, *Krox20*, *Hoxa2*, *follistatin*, and *kreisler* contribute to the establishment of the normal pattern of rhombomeres in the developing hindbrain. This model is described in detail below and summarized in Fig. 8.

It has been reported that the establishment of the *Hoxb1* expression in r4 depends on both *Hoxa1* and *Hoxb1* function (Studer et al., 1998). These authors showed that *Hoxb1* expression is initially activated in r4 of both *Hoxb1* (normal levels) and *Hoxa1* (weaker and reduced levels) mutant embryos, but was not activated in r4 of *Hoxa1/Hoxb1* double mutants. We extend these observations by showing that *Hoxa1* is required for the expression of *Hoxb1* in the anterior region of r4. We have demonstrated this finding by using both morphological and molecular markers. First, we provided evidence that *Hoxb1* expression was shifted posteriorly relative to morphological landmarks (i.e., the preotic sulcus and the r4 bulge). In addition, we demonstrated that in *Hoxa1gfp* mutant homozygotes, *Hoxb1* expression is shifted posteriorly relative to the anterior limit of the *Hoxa1gfp* expression domain (i.e.,

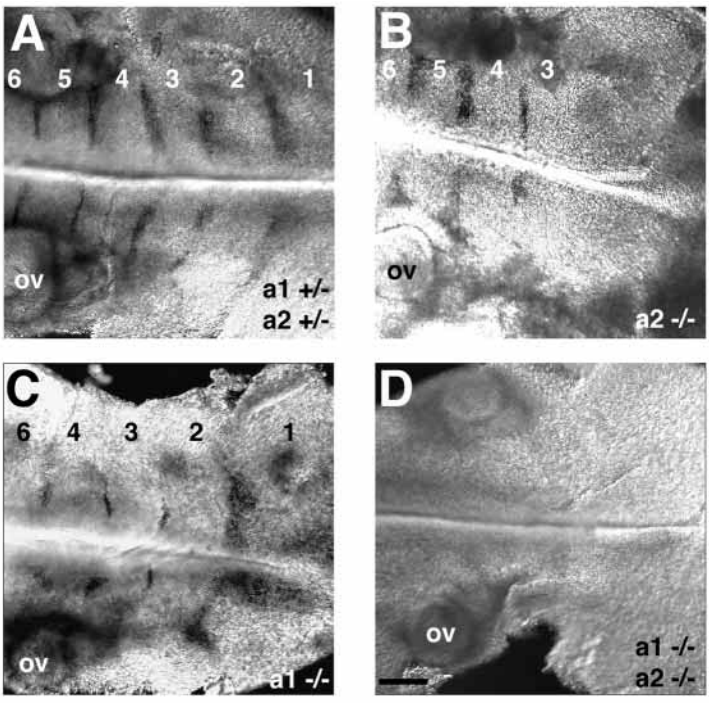

Fig. 7. Hindbrain segmentation. (A-D) Hindbrain flat mounts of approx. E10.25 hindbrains visualized by Nomarski optics. (A) Control embryo; note the rhombomere boundaries separating rhombomeres 1-6. The otic vesicle is at the level of r5. (B) *Hoxa2* mutant embryo; the r1/2 and r2/3 boundaries are absent. (C) *Hoxa1*$^{-/-}$ embryo; four boundaries are present. Based on marker analyses, we propose that the missing rhombomere is r5. The otic vesicle is at the level of r4. (D) *Hoxa1/Hoxa2* double mutant embryo; note the complete absence of rhombomere boundaries. Otic vesicle (ov). Scale bar is 200 μm.

r3/4; Fig. 2D-F). In contrast, in heterozygous (Fig. 2A-C) and control embryos (Murphy and Hill, 1991) the anterior limit of expression of both paralogs coincide at the r3/4 presumptive boundary. We also found that the *Hoxa1gfp* expression limit (r3/4) was approximately the same distance from the preotic sulcus in both *Hoxa1* mutant homozygous and heterozygous animals, demonstrating that this morphological landmark is at the same axial level in both mutants and controls.

The maintenance of *Hoxb1* expression in r4 after the regression of both *Hoxa1* and *Hoxb1* expression from the hindbrain is dependent on a *Hoxb1* auto-regulatory loop (Pöpperl et al., 1995). Interestingly, *kreisler* appears to play an important role in assuring that the autoregulated *Hoxb1* expression is restricted to r4. Thus in *kreisler* mutants, autoregulated *Hoxb1* expression is maintained ectopically in r5 (McKay et al., 1994). In mutants that lack *Hoxa1*, we have also observed that *Hoxb1* expression was maintained at the level of r5 suggesting that perhaps *kreisler* is misregulated in *Hoxa1* mutants. Indeed, we have found that in *Hoxa1* mutants, the *kreisler* expression domain has been reduced to the width of single rhombomere corresponding to the level of r6 (J. R. B., unpublished observations; Rossel and Capecchi, 1999; see also Fig. 2 of Gavalas et al., 1998). Thus, *Hoxa1* may be required to activate *kreisler* expression in r5.

Krox20 expression is initially activated in rhombomere 3 at E8.0. It commences as a narrow stripe of cells that expands rostrally with time (Fig. 1A-C; see also Irving et al., 1996). Slightly later in development (approx. E8.5), *Krox20* expression is activated in r5 in rostral to caudal fashion (Irving et al., 1996). It appears that the mechanisms that activate *Krox20* in rhombomeres 3 are different from those that activate it in r5. For example, previous work by Graham and Lumsden, (1996) demonstrate that r5 explants, whether cultured in isolation or transplanted to ectopic regions of the hindbrain, always express *Krox20*. In contrast, rhombomere 3, whether transplanted to ectopic regions in the hindbrain or cultured in isolation, fail to express it. Only in situations where r3 is adjacent to r4 in explant cultures is r3 found to express *Krox20*. Furthermore, work by Helmbacher et al. (1998) demonstrates that *Hoxa1* (expressed in r4 and more posteriorly) plays a synergistic role with *Krox20* in establishing *Krox20* expression in r3. Taken together, these results suggest that cells in r5 possess the intrinsic ability to express *Krox20*, whereas those in r3 appear to require signals from r4 in order to do so. We also have made similar observations in our experiments. For example, we have found that the region of the hindbrain that gives rise to rhombomeres 4 and 5 has the intrinsic ability to express *Krox20* provided that neither *Hoxa1* nor *Hoxb1* is expressed in these rhombomeres at the same time. Thus, in the case of *Hoxa1/Hoxb1* double mutants neither *Hoxa1* nor *Hoxb1* is expressed at the level of r4 or r5 and *Krox20* is expressed in these rhombomeres in their absence (Rossel and Capecchi, 1999). In addition, in wild-type embryos, *Krox20* is never expressed in r5 until after the retreat of *Hoxa1* and *Hoxb1* from this region of the hindbrain (Figs 1A-C, 3A). Interestingly, the activation of *Krox20* is in rostral to caudal fashion (Irving et al., 1996) mirroring the anterior to posterior retreat of the *Hox1* paralogs from this region. Further evidence of this phenomenon comes from *Hoxa1* mutants, where the anterior limit of *Hoxb1* expression is shifted to the caudal region of r4. Thus, neither *Hoxa1* nor *Hoxb1* is expressed in anterior r4 and *Krox20* expression is activated in this rhombomere in their absence. Finally, in *kreisler* and *Hoxa1* mutants, which allow ectopic, autoregulated expression of *Hoxb1* in r5, *Krox20* is never activated at this level (herein; McKay et al., 1994). We conclude, therefore that rhombomeres 4 and 5 are similar with respect to the activation of *Krox20* in that they possess the intrinsic ability to activate *Krox20* expression in the absence of *Hox1* paralogs.

Similar to previous work, we found that activation of *Krox20* at the level of rhombomere 3 was dependent on signals from r4. More specifically our work suggests that these signals are downstream from *Hoxa1* and *Hoxb1*. For example, in *Hoxa1* mutants we showed that there was a delay in the activation of *Krox20* expression in cells just posterior to the preotic sulcus (cells that should give rise to rhombomere 3). Thus at E8.0, in contrast to control embryos, *Hoxa1* mutants possess only a few *Krox20*-expressing cells at the level of r3. By E8.5, this number has expanded and by E8.75 the expansion appears to be complete. We propose that the delay in *Krox20* expression is due to the fact that the anterior limit of *Hoxb1* expression is found at a more posterior level. Thus, the proposed signal downstream of *Hoxb1* is activated in a more posterior domain of the hindbrain and must be propagated a further distance in order to reach the cells in r3 (i.e., the cells just posterior to the

preotic sulcus). In corroboration of this hypothesis, we have observed in *Hoxa1/Hoxb1* double mutants that the region just posterior to the preotic sulcus ('r3') is completely devoid of *Krox20* expression (Rossel and Capecchi, 1999), again demonstrating the requirement of the *Hox1* parologs for the activation of *Krox20* in r3. We therefore extend previous experiments (Graham and Lumsden, 1996; Helmabacher et al., 1998) by showing that *Hoxa1* and *Hoxb1*, two molecules essential for the formation of r4 (Rossel and Capecchi, 1999), are required to activate *Krox20* in r3.

We have shown that in *Hoxa1* mutants *Krox20* expression, although delayed, expands relatively normally in the r3 territory (Figs 1D, 3C,E). In *Hoxa1/Hoxa2* double mutants, however, this expansion is severely affected such that even by E8.75 there are very few *Krox20*-expressing cells at the level of r3 (Fig. 3F). Thus, while *Hoxa1* and *Hoxb1* play a role in the activation of *Krox20* in r3, *Hoxa2* appears to be important for the anterior expansion of this expression domain. It has been demonstrated previously that *Krox20* is required for *Hoxa2* expression in r3 (Nonchev et al., 1996). It is therefore not surprising that *Krox20* mutants appear to show a similar yet more severe defect in the expansion of rhombomere 3 identity (Schneider-Maunoury et al., 1993). In *Krox20* mutants, it has been demonstrated that *Krox20* is activated in the first few rows of cells in r3, just as in controls at E8.0 (Schneider-Maunoury et al., 1993). In contrast to controls, however, this thin band fails to expand (see fig. 2 of Schneider-Maunoury et al., 1993; fig. 4 of Seitanidou et al., 1997) indicating that as was the case with *Hoxa2*, *Krox20* appears to play an important role in the expansion of *Krox20*-expressing cells in r3.

It is interesting to note that in *Krox20* mutants, all of the cells in the r5 domain express *Krox20* (Schneider-Maunoury et al., 1993), again highlighting the fact that cells at the level of r5 possess the intrinsic ability to activate *Krox20*. These cells, however, do not express *Krox20* until E8.5 (after the retreat of the *Hox1* paralogs). In contrast, in r3 of the *Krox20* mutants, only the first few rows of cells are activated; an expected result given that *Hoxa1* and *Hoxb1* are still present in r4 to activate these cells (via downstream signals).

Follistatin is activated very early in the neural plate (Albano et al., 1994). Prior to E8.0 it is presumably expressed as a solid band from r2-r4. Following E8.0, there is a band of nonexpressing cells at the level of r3 which now separates the *follistatin* expression domain into an r2 and an r4 band. This band of nonexpressing cells corresponds to the *Krox20* expression domain. Interestingly, Seitanidou et al. (1997) have demonstrated that in *Krox20* mutants that *follistatin* is expressed as a solid domain from r2 to r4, demonstrating that *Krox20* represses *follistatin* in r3. In *Hoxa1* and *Hoxa1/Hoxa2* mutants the pattern of *Krox20* has been significantly altered. It comes as no surprise, therefore, that we see concomitant changes in *follistatin* expression in these mutant backgrounds. Thus, a large nonexpressing domain separating the two *follistatin* expression stripes is observed in *Hoxa1* mutants, corresponding to the large *Krox20* expression domain in r3 and anterior r4 (Fig. 4G). Not surprisingly, the posterior *follistatin-expressing* band was very thin, demonstrating that the *Krox20* domain extends ectopically into most of rhombomere 4. It is interesting to note that in *Hoxa1/Hoxa2* double mutants, due to the delay of *Krox20* expansion into r3, *follistatin* is not repressed in this region (Fig. 4H) and thus the expression of r2-specific markers is permitted at this level (see also Fig. 4D).

Neuregulin is expressed in two stripes in mutants lacking *Hoxa1*, similar to controls; however, we find that the second stripe, which typically rests directly above the 2nd arch and anterior to the invaginating otic placode, is now located posterior to the 2nd arch and immediately adjacent to the otic placode (Fig. 4C). This observation provides further evidence that r4 markers are expressed at the level of r5 in *Hoxa1* mutants.

We propose the following model for how *Hoxa1*, *Hoxb1*, *Krox20*, *Hoxa2*, *kreisler*, and *follistatin* function together to establish the normal pattern of rhombomeres 2-6 in the early hindbrain (see Fig. 8). Prior to E8.0, *Hoxa1* and *Hoxb1* are expressed throughout the neural plate and form a sharp anterior limit at the r3/4 presumptive boundary, while *follistatin* is expressed in presumptive rhombomeres 2-4. The expression of *Hoxa1* is required to activate *Hoxb1* in the anterior regions of r4. By E8.0, *Hoxa1* and *Hoxb1* have activated the transcription of other r4-specific genes including a downstream signal that induces *Krox20* expression in the first 3-4 rows of cells in presumptive r3 (Fig. 8A). Once activated, *Krox20* activates downstream targets, including *Hoxa2* and *Hoxb2*, while repressing *follistatin*. The expansion of *Krox20* in r3 is dependent on its own expression and that of its downstream target(s), *Hoxa2* (and perhaps *Hoxb2*).

While still expressed in r5 (prior to E8.5), *Hoxa1* not only represses *Krox20* but is required to activate strong *kreisler* expression. By E8.5, the expression of both *Hox1* paralogs has regressed from the hindbrain except for the strong autoregulatory *Hoxb1* expression in r4. No longer repressed by *Hoxa1* and *Hoxb1*, *Krox20* is now activated throughout r5 (Fig. 8B) commencing with the most anterior cells (see Irving et al., 1996). The net result is strong expression of *Krox20* in r3 and r5 and *Hoxb1* in r4 (Fig. 8B). In addition, *kreisler* is expressed in r5 (thanks to the function of *Hoxa1*) and in r6. Finally *follistatin*, which commenced as a solid band of expression in presumptive r2-r4 prior to E8.0, is now separated into two domains of expression in r2 and r4 due to *Krox20* expression in r3.

In the absence of *Hoxa1*, the anterior limit of *Hoxb1* is established in the posterior region of r4 (Fig. 8A; *a1–/–* and *a1/a2–/–*). Several consequences result from this defect. First, without *Hoxa1* and *Hoxb1* in anterior r4, *Krox20* is no longer repressed at this level. Secondly, the putative downstream signaling molecule must be propagated further to reach r3, causing a delay in the induction of *Krox20* in r3. In addition, in the absence of *Hoxa1*, *kreisler* expression is not activated in r5. By E8.5 the expansion of *Krox20* in r3, although delayed, has commenced in *Hoxa1* single mutants (Fig. 8B *a1–/–*). Because *Krox20* and its downstream targets are present in the single mutants, the expansion proceeds relatively normally. In *Hoxa1/Hoxa2* double mutants, *Krox20*-expressing cells are induced sparingly in the region just posterior to the preotic sulcus (i.e., 'r3') (Fig. 8A, *a1a2–/–*) similar to *Hoxa1* single mutants; however, due to the absence of *Hoxa2*, expansion of *Krox20*-expressing cells in r3 is severely limited (Fig. 8B, *a1a2–/–*). Due to the severe delay of *Krox20* expression in 'r3', *follistatin* is not repressed and thus this region takes on an r2 identity.

By E8.5 for both mutant classes, *Hoxb1* expression has

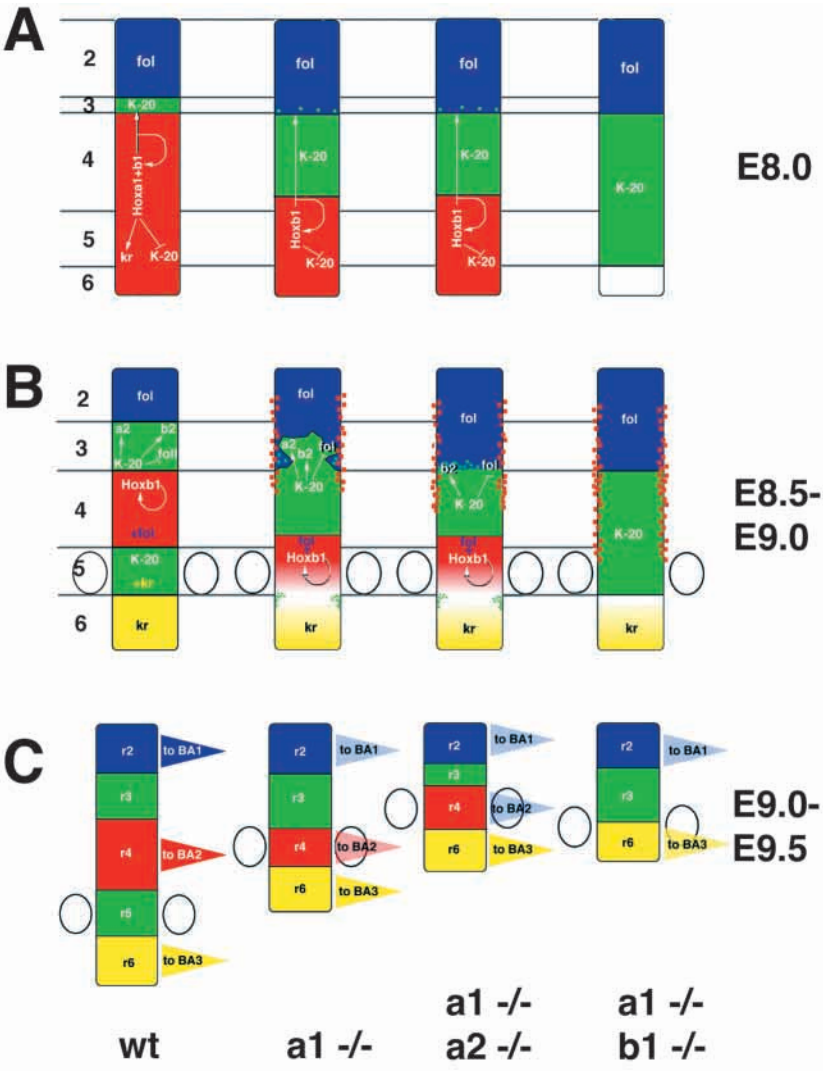

Fig. 8. Schematic representation of embryonic hindbrains from E8.0-E9.5. (A, wt) *Hoxa1* and *Hoxb1* (red) are coexpressed up to the presumptive r3/4 boundary. *Hoxa1* is required to establish *Hoxb1* expression in anterior r4. *Hoxa1* and *Hoxb1* activate the transcription of r4-specific downstream targets including a signal (upward arrow) which in turn induces *Krox20* (K-20; green) expression in cells just anterior to the r3/4 boundary (in cells that are not expressing *Hoxa1* or *Hoxb1*). *Krox20* is repressed, however, in r4 and r5 cells that are expressing *Hoxa1* and *Hoxb1*. *Hoxa1* is required for *kreisler* (kr) expression in r5. (A, a1 –/– and a1/a2 –/–) Without *Hoxa1*, the anterior limit of *Hoxb1* is established in the posterior region of r4. Because of this posterior shift, neither *Hoxa1* nor *Hoxb1* is expressed in the anterior portion of r4 and *Krox20* is no longer repressed there. Furthermore, the signal downstream of *Hoxb1* (upward arrow) must be propagated a longer distance causing a delay in the induction of *Krox20* expression in presumptive r3. Due to the absence of *Hoxa1*, *kreisler* expression is not activated in r5. (A, a1/b1 –/–) Without *Hoxa1* and *Hoxb1* expression, *Krox20* expression is no longer repressed in r4 and r5. In addition, the signal downstream from *Hoxa1* and *Hoxb1* required to induce *Krox20* expression in r3 is not activated. (B, wt) By E8.5, *Hoxa1* expression has completely retreated from the hindbrain. *Hoxb1* has also retreated with the exception of the strong autoregulatory expression in r4. Once *Hoxa1* and *Hoxb1* expression has fully retreated from r5, *Krox20* expression commences at this level. *Krox20* expression also expands into r3. This expansion requires activation of its downstream target *Hoxa2* and possibly *Hoxb2*. Strong *kreisler* expression in r5 maintains *Hoxb1* autoregulated expression at the r4/5 boundary. (B, a1 –/–) *Hoxb1* expression retreats from the caudal hindbrain leaving autoregulated expression in caudal r4. Because *kreisler* is not activated in r5, autoregulated *Hoxb1* expression extends into r5 as well. *Krox20* expansion into r3 although delayed (due to the fewer number of cells that were induced at E8.0) occurs somewhat normally due to the fact that *Krox20* and its downstream targets *Hoxa2* and perhaps *Hoxb2* are functioning. As a consequence of the larger expression domains of *follistatin* (r2 and part of r3) and *Krox20* (part of r3 and r4), a regulatory event driven by apoptosis (orange dots), commences in these regions of the neural tube. (B, a1/a2 –/–) The hindbrain is similar to that of *Hoxa1* single mutants except that *Krox20* expansion into r3 is severely delayed. *Hoxa2* is a downstream target of *Krox20* and if absent, cripples the expansion of *Krox20*-expressing cells into r3. (B, a1/b1 –/–) *Krox20* is never induced in r3 and thus never expands into r3. As a result, *follistatin* expression extends to the r3/r4 boundary (M. Rossel and MRC, unpublished results). Due to enlarged *follistatin* and *Krox20*-expressing domains, apoptosis is activated in the neural tube at this level. (C, wt) A normal hindbrain with neural crest emanating from even numbered rhombomeres to their appropriate branchial arch. (C, a1–/–) Due to the apoptosis at the levels of r2 and r3, there is not only a reduction in the number of neural crest (symbolized by the light blue color) that will populate the first arch, but also the abnormally large r3 is reduced to almost normal proportions. There is also a reduction in the number of neural crest that reach the second arch (light red) due to the reduced size of r4 and the fact that the otocyst may act as a barrier to prevent normal migration of the crest. The otocysts do not shift anteriorly to the level of r4, instead r4 is specified more posteriorly (at the level of the otocysts). (C, a1/a2 –/–) Very similar to *Hoxa1* single mutants except that, due to the lack of *Hoxa2*, the r4 neural crest has taken on an r1/r2 identity (blue). In addition, the lack of *Hoxa1* causes a reduction in r4 neural crest (indicated by light blue) contributing to the second arch. (D, a1/b1 –/–) r4 is never specified. Therefore, there is no r4 neural crest to populate the second arch.

retreated from the hindbrain leaving only autoregulated *Hoxb1* expression in posterior r4. In addition, due to the absence of *kreisler* in r5, autoregulatory *Hoxb1* expression extends into r5 which represses the expression of *Krox20* at this level. Thus, r4 specific genes are expressed at the level of r5, transforming this region to an r4 identity (similar to the scenario in *kreisler* mutants).

Without the function of either of the *Hox1* paralogs in the developing hindbrain of E8.0 embryos, several consequences would be predicted to ensue. First, *Krox20* expression would be derepressed at the level of both r4 and r5 (*a1b1–/–*, Fig. 8A). Second, the signal downstream of *Hoxa1* and *Hoxb1* would never be activated and thus *Krox20* expression would not be induced in the region of the hindbrain that should give

rise to r3 (Fig. 8A). Third, because *Krox20* expression is not activated in r3, *follistatin* expression is not repressed at this level transforming this region to an r2 identity. Finally, as was the case with the other mutant classes lacking *Hoxa1*, *kreisler* expression would not be activated in r5. All of these predictions have been observed in *Hoxa1/Hoxb1* double mutant embryos (Rossel and Capecchi, 1999 and data not shown).

Later hindbrain patterning

Early on, *Hoxa1* mutants have an extended *Krox20* expression domain. We suggest that extension of the r3-*Krox20* domain results from part of r4 being transformed to an r3 fate. A similar finding was reported by McKay et al. (1994) for *kreisler* mutants where at early stages the 5th rhombomere appears to take on an r4 identity. Thus, the region of the hindbrain expressing *Hoxb1* is larger than normal and by E9.5 they observed an elevation of cell death in r4. They proposed that an intrinsic mechanism exists in the embryo that regulates the abnormally large size of the 'r4' segment via apoptosis. We report a similar phenomenon at the level of r2 and r3 in mutants lacking *Hoxa1*. Ectopic apoptosis is induced in the r2-r3 region as a means of regulating the larger *follistatin*-expressing domain in r2 (due to the delay of *Krox20* expansion into r3) and that of *Krox20* in the r3-4 region (due to the derepression of *Krox20* in r4; see Fig. 8B).

Conclusion

We have presented evidence that *Hoxa1* is required to establish the expression of *Hoxb1* to the normal presumptive r3/4 boundary. Failure to do so not only affects the identity of r4, but also delays the specification of r3. We provide evidence, as have others (Helmbacher et al., 1998), that the expansion of r3 identity is also dependent on *Krox20* and its downstream targets. We suggest that *Hoxa1* may be required for *kreisler* expression in r5. Without *kreisler* at this level, autoregulatory *Hoxb1* expression is allowed to extend into r5, changing its fate to an r4 identity as seen in *kreisler* mutants. Thus, we propose that in mutants lacking *Hoxa1*, the region of the hindbrain that normally gives rise to r4 and r5 has been anteriorly transformed to an r3 and r4 identity, respectively. *Drosophila* embryos lacking *HOM-C* gene function, also exhibit anterior transformations in the identity of parasegments, demonstrating an evolutionarily conserved role among insects and vertebrates for *Antennapedia* class transcription factors during embryogenesis (reviewed in McGinnis and Krumlauf, 1992). Unlike the fruit fly, which treats homeotically duplicated segments as separate compartments, the mouse (and perhaps all vertebrates) considers the duplicated area as one unusually large segment and subsequently regulates its size via apoptosis. This apoptotic process may play an important role in regulating the size of rhombomeres during normal development. Finally, we have provided evidence that the early patterning defects and subsequent remodeling of the mutant hindbrains underlie the abnormalities observed in the organization of compartments in the mutant hindbrains.

We thank P. Charnay, J. C. Smith, C. Birchmeier for the *EphA4*, *follistatin* and *neuregulin* in situ probes, respectively. J. R. B. was supported by an NIH Developmental Biology Training Grant (5T32 HD07491).

REFERENCES

Albano, R. M., Arkell, R., Beddington, R. S. and Smith, J. C. (1994). Expression of inhibin subunits and *follistatin* during postimplantation mouse development: decidual expression of activin and expession of folistatin in primitive streak, somites and hindbrain. *Development* **120**, 803-813.

Barrow, J. R. and Capecchi, M. R. (1996). Targeted disruption of the *hoxb-2* locus in mice interferes with expression of *hoxb-1* and *hoxb-4*. *Development* **122**, 3817-3828.

Barrow, J. R. and Capecchi, M. R. (1999). Compensatory defects associated with mutations in *Hoxa1* restore normal palatogenesis to *Hoxa2* mutants. *Development* **126**, 5011-5026.

Carpenter, E. M., Goddard, J. M., Chisaka, O., Manley, N. R. and Capecchi, M. R. (1993). Loss of *Hox-A1* (*Hox-1.6*) function results in the reorganization of the murine hindbrain. *Development* **118**, 1063-1075.

Chisaka, O., Musci, T. S. and Capecchi, M. R. (1992). Developmental defects of the ear, cranial nerves and hindbrain resulting from targeted disruption of the mouse homeobox gene *Hox-1.6*. *Nature* **355**, 516-520.

Fraser, S., Keynes, R. and Lumsden, A. (1990). Segmentation in the chick embryo hindbrain is defined by cell lineage restrictions. *Nature* **344**, 431-435.

Frohman, M. A., Boyle, M. and Martin, G. R. (1990). Isolation of the mouse *Hox-2.9* gene; analysis of embryonic expression suggests that positional information along the anterior-posterior axis is specified by mesoderm. *Development* **110**, 589-607.

Frohman, M. A., Martin, G. R., Cordes, S. P., Halamek, L. P. and Barsh, G. S. (1993). Altered rhombomere-specific gene expression and hyoid bone differentiation in the mouse segmentation mutant, *kreisler (kr)*. *Development* **117**, 925-936.

Gavalas, A., Davenne, M., Lumsden, A., Chambon, P. and Rijli, F. M. (1997). Control of axon guidance and rostral hindbrain patterning by *Hoxa2*. *Development* **124**, 3693-3702.

Gavalas, A., Studer, M., Lumsden, A., Rijli, F. M., Krumlauf, R. and Chambon, P. (1998). *Hoxa1* and *Hoxb1* synergize in patterning the hindbrain, cranial nerves and second pharyngeal arch. *Development* **125**, 1123-1136.

Gendron-Maguire, M., Mallo, M., Zhang, M. and Gridley, T. (1993). *Hoxa-2* mutant mice exhibit homeotic transformation of skeletal elements derived from cranial neural crest. *Cell* **75**, 1317-1331.

Gilardi-Hebenstreit, P., Nieto, M. A., Frain, M., Mattei, M.-G., Chestier, A., Wilkinson, D. G. and Charnay, P. (1992). An *Eph*-related receptor protein tyrosine kinase gene segmentally expressed in the developing mouse hindbrain. *Oncogene* **7**, 2499-2506.

Goddard, J. M., Rossel, M., Manley, N. R. and Capecchi, M. R. (1996). Mice with targeted disruption of *Hoxb-1* fail to form the motor nucleus of the VIIth nerve. *Development* **122**, 3217-3228.

Godwin, A.R., Stadler, H. S., Nakamura, K., Capecchi, M. R. (1998) Detection of targeted *GFP-Hox* gene fusions during mouse embryogenesis. *Proc. Natl. Acad. Sci. USA* **95**, 13042-13047.

Graham, A. and Lumsden, A. (1996). Interactions between rhombomeres modulate *Krox20* and *follistatin* expression in the chick embryo hindbrain. *Development* **122**, 473-480.

Helmbacher, F., Pujades, C., Desmarquet, C., Frain, M., Rijli, F. M., Chambon, P. and Charnay, P. (1998). *Hoxa1* and *Krox20* synergize to control the development of rhombomere 3. *Development* **125**, 4739-4748.

Hunt, P., Gulisano, M., Cook, M., Sham, M.-H., Faiella, A., Wilkinson, D., Boncinelli, E. and Krumlauf, R. (1991a). A distinct *Hox* code for the branchial region of the vertebrate head. *Nature* **353**, 861-864.

Hunt, P., Whiting, J., Nonchev, S., Sham, M.-H., Marshall, H., Graham, A., Cook, M., Allemann, R., Rigby, P. W. J., Gulisano, M., Faiella, A., Boncinelli, E. and Krumlauf, R. (1991b). The branchial *Hox* code and its implications for gene regulation, patterning of the nervous system and head evolution. *Development* **Supplement 2**, 63-77.

Irving, C., Nieto, M. A., DasGupta, R., Charnay, P. and Wilkinson, D. G. (1996). Progressive spatial restriction of *Sek-1* and *Krox20* gene expression during hindbrain segmentation. *Dev. Biol.* **173**, 26-38.

Köntges, G. and Lumsden, A. (1996). Rhombencephalic neural crest segmentation is preserved throughout craniofacial ontogeny. *Development* **122**, 3229-3242.

Lufkin, T., Dierich, A., LeMeur, M., Mark, M. and Chambon, P. (1991). Disruption of the *Hox-1.6* homeobox gene results in defects in a region corresponding to its rostral domain of expression. *Cell* **66**, 1105-1119.

Lumsden, A. and Keynes, R. (1989). Segmental patterns of neuronal development in the chick hindbrain. *Nature* **337**, 424-428.

Manley, N. R. and Capecchi, M. R. (1995). The role of *hoxa-3* in mouse thymus and thyroid development. *Development* **121**, 1989-2003.

Mark, M., Lufkin, T., Vonesch, J.-L., Ruberte, E., Olivo, J.-C., Dollé, P., Gorry, P., Lumsden, A. and Chambon, P. (1993). Two rhombomeres are altered in *Hoxa-1* mutant mice. *Development* **119**, 319-338.

McGinnis, W. and Krumlauf, R. (1992). Homeobox genes and axial patterning. *Cell* **68**, 283-302.

McKay, I. J., Muchamore, I., Krumlauf, R., Maden, M., Lumsden, A. and Lewis, J. (1994). The *kreisler* mouse: a hindbrain segmentation mutant that lacks two rhombomeres. *Development* **121**, 2199-2211.

Meyer, D., Yamaai, T., Garratt, A., Riethmacher-Sonnenberg, E., Kane, D., Theill, L. E. and Birchmeier, C. (1997). Isoform-specific expression and function of neuregulin. *Development* **124**, 3575-3586.

Murphy, P. and Hill, R. E. (1991). Expression of the mouse *labial*-like homeobox-containing genes, *Hox-2.9* and *Hox-1.6*, during segmentation of the hindbrain. *Development* **111**, 61-74.

Nonchev, S., Vesque, C., Maconochie, M., Seitanidou, T., Ariza-McNaughton, L., Frain, M., Marshall, H., Sham, M. H., Krumlauf, R. and Charnay, P. (1996). Segmental expression of *Hoxa-2* in the hindbrain is directly regulated by *Krox 20*. *Development* **122**, 543-554.

Pöpperl, H., Bienz, M., Studer, M., Chan, S.-K., Aparicio, S., Brenner, S., Mann, R. S., Krumlauf, R. (1995). Segmental expression of *Hoxb-1* is controlled by a highly conserved autoregulatory loop dependent upon *exd/pbx*. *Cell* **81**, 1031-1042.

Rijli, F. M., Mark, M., Lakkaraju, S., Dierich, A., Dollé, P. and Chambon, P. (1993). A homeotic transformation is generated in the rostral branchial region of the head by disruption of *Hoxa-2*, which acts as a selector gene. *Cell* **75**, 1333-1349.

Rossel, M. and Capecchi, M. R. (1999). Mice mutant for both *Hoxa1* and *Hoxb1* show extensive remodeling of the hindbrain and defects in craniofacial development. *Development* **126**, 5027-5040.

Schneider-Maunoury, S., Topilko, P., Seitanidou, T., Levi, G., Cohen-Tannoudji, M., Pournin, S., Babinet, C. and Charnay, P. (1993). Disruption of *Krox20* results in alteration of rhombomeres 3 and 5 in the developing hindbrain. *Cell* **75**, 1199-1214.

Schwenk, F., Baron, U., and Rajewsky, K. (1995). A *cre*-transgenic mouse strain for the ubiquitous deletion of *loxP*-flanked gene segments including deletion in germ cells. *Nucleic Acids Res.* **23,** 5080-5081.

Seitanidou, T., Schneider-Maunoury, S., Desmarquet, C., Wilkinson, D. G. and Charnay, P. (1997). *Krox20* is a key regulator of rhombomere-specific gene expression in the developing hindbrain. *Mech. Dev.* **65**, 31-42.

Sham, M. H., Vesque, C., Nonchev, S., Marshall, H., Frain, M., Gupta, R. D., Whiting, J., Wilkinson, D., Charnay, P. and Krumlauf, R. (1993). The zinc finger gene *Krox20* regulates *HoxB2* (*Hox2.8)* during hindbrain segmentation. *Cell* **72**, 183-196.

Studer, M., Gavalas, A., Marshall, H., Ariza-McNaughton, L., Rijli, F. M., Chambon, P. and Krumlauf, R. (1998). Genetic interactions between *Hoxa1* and *Hoxb1* reveal new roles in regulation of early hindbrain patterning. *Development* **125**, 1025-1036.

Studer, M., Lumsden, A., Ariza-McNaughton, L., Bradley, A. and Krumlauf, R. (1996). Altered segmental identity and abnormal migration of motor neurons in mice lacking *Hoxb-1*. *Nature* **384**, 630-634.

Trainor, P. A. and Tam, P. P. (1995). Cranial paraxial mesoderm and neural crest cells of the mouse embryo: co-distribution in the craniofacial mesenchyme but distinct segregation in branchial arches. *Development* **121**, 2569-2582.

Wilkinson, D. G., Bhatt, S., Chavrier, P., Bravo, R. and Charnay, P. (1989). Segment-specific expression of a zinc-finger gene in the developing nervous system of the mouse. *Nature* **337**, 461-464.

Zhang, M., Kim, H.-J., Marshall, H., Gendron-Maguire, M., Lucas, D. A., Baron, A., Gudas, L. J., Gridley, T., Krumlauf, R. and Grippo, J. F. (1994). Ectopic *Hoxa-1* induces rhombomere transformation in the mouse hindbrain. *Development* **120**, 2431-2442.